

# A combination of Residual Distribution and the Active Flux formulations or a new class of schemes that can combine several writings of the same hyperbolic problem: application to the 1D Euler equations

R. Abgrall

Institute of Mathematics, University of Zürich  
Wintherhurerstrasse 190, CH 8057 Zürich

November 26, 2020

## Abstract

We show how to combine in a natural way (i.e. without any test nor switch) the conservative and non conservative formulations of an hyperbolic system that has a conservative form. This is inspired from two different class of schemes: the Residual Distribution one, and the Active Flux formulations. This new class of scheme is proved to satisfy a Lax-Wendroff like theorem. We also develop a method to perform non linear stability. We illustrate the behaviour on several benchmarks, some quite challenging.

## 1 Introduction

The notion of conservation is essential in the numerical approximation of hyperbolic systems of conservation: if it is violated, there is no chance, in practice, to compute the right weak solution in the limit of mesh refinement. This statement is known since the celebrated work of Lax and Wendroff [1], and what happens when conservation is violated has been discussed by Hou and Le Floch [2]. This conservation requirement impose the use of the conservation form of the system. However, in many practical situation, this is not really the one one would like to deal with, since in addition to conservation constraints, one also seeks for the preservation of additional features, like contacts for fluid mechanics, or entropy decrease for shocks.

In this paper, we are interested in compressible fluid dynamics. Several authors have already considered the problem of the correct discretisation of the non conservative form of the system. In the purely Lagrangian framework, when the system is described by the momentum equation and the Gibbs equality, this has been done since decades: one can consider the seminal work of Wilkins, to begin with, and the problem is still of interest: one can consider [3, 4, 5] where high order is sought for. In the case of the Eulerian formulation, there are less work. One can mention [6, 7, 8] where staggered meshes are used, the thermodynamic variables are localised in the cells, while the kinetic ones are localised at the grid points, or [9] where a non conservative formulation with correction is used from scratch. The first two references show how to construct at most second order scheme, while the last one shows this for any order. All constructions are quite involved in term of algebra, because one has to transfert information from the original grid and the staggered one.

In this paper, we aim at showing how the notion of conservation introduced in the residual distribution framework [10] is flexible enough to allow to deal directly with the non conservative form of the system, while the correct solutions are obtained in the limit of mesh refinement. More precisely, we show how to deal both with the conservative and non conservative form of the PDE, without any switch, as it was the case in [11]. We illustrate our strategy on several versions of the non conservative form, and provide first, second order and third order accurate version of the scheme. More than a particular example, we describe

a general strategy which is quite simple. The systems on which we will work are descriptions of the Euler equations for fluid mechanics:

- The conservation one:

$$\frac{\partial}{\partial t} \begin{pmatrix} \rho \\ \rho u \\ E \end{pmatrix} + \frac{\partial}{\partial x} \begin{pmatrix} \rho u \\ \rho u^2 + p \\ u(E + p) \end{pmatrix} = 0 \quad (1)$$

- the primitive formulation:

$$\frac{\partial}{\partial t} \begin{pmatrix} \rho \\ u \\ p \end{pmatrix} + \begin{pmatrix} \frac{\partial \rho u}{\partial x} \\ u \frac{\partial u}{\partial x} + \frac{1}{\rho} \frac{\partial p}{\partial x} \\ u \frac{\partial p}{\partial x} + (e + p) \frac{\partial u}{\partial x} \end{pmatrix} = 0 \quad (2)$$

- The "entropy" formulation:

$$\frac{\partial}{\partial t} \begin{pmatrix} p \\ u \\ s \end{pmatrix} + \begin{pmatrix} u \frac{\partial p}{\partial x} + (e + p) \frac{\partial u}{\partial x} \\ u \frac{\partial u}{\partial x} + \frac{1}{\rho} \frac{\partial p}{\partial x} \\ u \frac{\partial s}{\partial x} \end{pmatrix} = 0 \quad (3)$$

where as usual  $\rho$  is the density,  $u$  the velocity,  $p$  the pressure,  $E = e + \frac{1}{2}\rho u^2$  is the total energy,  $e = (\gamma - 1)p$  and  $s = \log(p) - \gamma \log(\rho)$  is the entropy.

This paper has several source of inspirations. The first one is the residual distribution (RD) framework, and in particular [10]. The second one is the family of active flux [12, 13, 14, 15, 16], where the solution is represented by a cell average and point values. The conservation is recovered from how the average is updated. Here the difference comes from the fact that in addition several systems can be conserved while a Lax Wendroff like result can still be shown. If the same system were used, both for the cell average and the point values, this would easily fit into the RD framework, using the structure of the polynomial reconstruction. The difference with Active Flux is that we use only the representation of the solution within one cell, and not a fancy flux evaluation.

The format of the paper is as follow. In a first part, we explain the general principles of our method, and justify why, under the assumptions made on the numerical sequence for the Lax-Wendroff theorem (boundedness in  $L^\infty$  and strong convergence in a  $L^p$ ,  $p \geq 1$ , of a subsequence toward a  $v \in L^p$ , then this  $v$  is a weak solution of the problem), we also have the same property here. In the second part, we describe several discretisation of the method, and in a third part we provide several simulation to illustrate the method.

## 2 The method

### 2.1 Principle

We consider the problem

$$\frac{\partial \mathbf{u}}{\partial t} + \frac{\partial \mathbf{f}(\mathbf{u})}{\partial x} = 0, \quad x \in \mathbb{R} \quad (4a)$$

with the initial condition

$$\mathbf{u}(x, 0) = \mathbf{u}_0(x), \quad x \in \mathbb{R} \quad (4b)$$

Here  $\mathbf{u} \in \mathcal{D}_{\mathbf{u}} \subset \mathbb{R}^p$ . For smooth solutions, we also consider an equivalent formulation in the form

$$\frac{\partial \mathbf{v}}{\partial t} + J \frac{\partial \mathbf{v}}{\partial x} = 0 \quad (4c)$$

where  $\mathbf{v} = \Psi(\mathbf{u}) \in \mathcal{D}_{\mathbf{v}}$  and  $\Psi : \mathcal{D}_{\mathbf{u}} \rightarrow \mathcal{D}_{\mathbf{v}}$  is assumed to be one-to-one. For example, if (4) corresponds to (1), then

$$\mathcal{D}_{\mathbf{u}} = \{(\rho, \rho u, E) \in \mathbb{R}^3 \text{ such that } \rho > 0 \text{ and } E - \frac{1}{2}\rho u^2 > 0\}.$$

If (4c) corresponds to (2), then

$$\mathcal{D}_{\mathbf{v}} = \{(\rho, u, p) \text{ such that } \rho > 0 \text{ and } p > 0\}$$

and (for a perfect gas) the mapping  $\Psi$  corresponds to  $(\rho, \rho u, E) \mapsto (\rho, u, p = (\gamma - 1)(E - \frac{1}{2}\rho u^2))$ , while

$$J = \begin{pmatrix} u & \rho & 0 \\ 0 & u & \frac{1}{\rho} \\ 0 & (e + p) & u \end{pmatrix}.$$

More generally, we have  $J = [\nabla_{\mathbf{u}}(\Psi^{-1})]\nabla_{\mathbf{u}}\mathbf{f}$ .

The idea is to discretise *simultaneously* (4a) and (4c). Forgetting the possible boundary conditions,  $\mathbb{R}$  is divided into non overlapping intervals  $K_{j+1/2} = [x_j, x_{j+1}]$  where  $x_j < x_{j+1}$  for all  $j \in \mathbb{Z}$ . We set  $\Delta_{j+1/2} = x_{j+1} - x_j$ . At the grid points, we will estimate  $\mathbf{v}_j$  in time, while in the cells we will estimate the average value

$$\bar{\mathbf{u}}_{j+1/2} = \frac{1}{\Delta_{j+1/2}} \int_{x_j}^{x_{j+1}} \mathbf{u}(x) dx$$

When needed, we have  $\mathbf{u}_j = \Psi^{-1}(\mathbf{v}_j)$ , however  $\bar{\mathbf{v}}_{j+1/2} = \Psi(\bar{\mathbf{u}}_{j+1/2})$  is meaningless since the  $\Psi$  does not commute with the average.

In  $K_{j+1/2}$  any continuous function can be represented by  $\mathbf{u}_j = \mathbf{u}(x_j)$ ,  $\mathbf{u}_{j+1} = \mathbf{u}(x_{j+1})$  and  $\bar{\mathbf{u}}_{j+1/2}$ : one can consider the following polynomial

$$R_{j+1/2}(x) = \mathbf{u}_j L_{j+1/2}^0 + \mathbf{u}_{j+1} L_{j+1/2}^1 + \bar{\mathbf{u}}_{j+1/2} L_{j+1/2}^{1/2},$$

with

$$L_{j+1/2}^\xi(x) = \ell_\xi\left(\frac{x - x_j}{x_{j+1} - x_j}\right)$$

and

$$\ell_0(s) = (1 - s)(1 - 3s), \quad \ell_1(s) = s(3s - 2), \quad \ell_{1/2}(x) = 6s(1 - s).$$

We see that

$$\begin{aligned} \ell_0(0) &= 1, \quad \ell_0(1) = 0, \quad \int_0^1 \ell_0(s) ds = 0 \\ \ell_1(1) &= 1, \quad \ell_1(0) = 0, \quad \int_0^1 \ell_1(s) ds = 0 \\ \int_0^1 \ell_{1/2}(s) ds &= 1, \quad \ell_{1/2}(0) = \ell_{1/2}(1) = 0. \end{aligned}$$

How to evolve  $\bar{\mathbf{u}}_{j+1/2}$  following (4a) and  $v_j$  following (4c) in time? The solution is simple for the average value: since

$$\Delta_{j+1/2} \frac{d\bar{\mathbf{u}}_{j+1/2}}{dt} + \mathbf{f}(\mathbf{u}_{j+1}(t)) - \mathbf{f}(\mathbf{u}_j(t)) = 0,$$

we simply take

$$\Delta_{j+1/2} \frac{d\bar{\mathbf{u}}_{j+1/2}}{dt} + (\hat{\mathbf{f}}_{j+1/2} - \hat{\mathbf{f}}_{j-1/2}) = 0 \tag{5}$$

where  $\hat{\mathbf{f}}_{j+1/2}$  is a numerical flux that depends continuously of its arguments. In practice, we take

$$\hat{\mathbf{f}}_{j+1/2} = \mathbf{f}(\mathbf{u}_j). \quad (6a)$$

For  $\mathbf{v}$ , we assume a semi-discrete scheme of the following form:

$$\Delta x \frac{d\mathbf{v}_j}{dt} + \overleftarrow{\Phi}_{j+1/2}^{\mathbf{v}} + \overrightarrow{\Phi}_{j-1/2}^{\mathbf{v}} = 0 \quad (6b)$$

such that  $\overleftarrow{\Phi}_{j+1/2}^{\mathbf{v}} + \overrightarrow{\Phi}_{j-1/2}^{\mathbf{v}}$  is a consistent approximation of  $J \frac{\partial \mathbf{v}}{\partial x}$ . We will give examples later, for now we only describe the principles. In general the residuals  $\overleftarrow{\Phi}_{j+1/2}^{\mathbf{v}}$  and  $\overrightarrow{\Phi}_{j-1/2}^{\mathbf{v}}$  need to depend on some  $\mathbf{v}_l$  and  $\mathbf{v}_{k+1/2} \approx \mathbf{v}(x_{l+1/2})$ . We can recover the missing informations at the half points in two steps:

1. From  $v_j$ , we can get  $\mathbf{u}_j = \Psi(\mathbf{v}_j)$ ,
2. Then in  $[x_j, x_{j+1}]$  we approximate  $\mathbf{u}$  by

$$R_{\mathbf{u}}(x) = \mathbf{u}_j \ell_0 \left( \frac{x - x_j}{\Delta_{j+1/2}} \right) + \bar{\mathbf{u}}_{j+1/2} \ell_{1/2} \left( \frac{x - x_j}{\Delta_{j+1/2}} \right) + \mathbf{u}_{j+1} \ell_1 \left( \frac{x - x_j}{\Delta_{j+1/2}} \right),$$

which enable to provide  $\mathbf{u}_{j+1/2} := R_{\mathbf{u}}(x_{j+1/2})$ , i.e

$$\mathbf{u}_{j+1/2} = \frac{3}{2} \bar{\mathbf{u}}_{j+1/2} - \frac{\mathbf{u}_j + \mathbf{u}_{j+1}}{4}. \quad (6c)$$

Note that this relation is simply  $\bar{\mathbf{u}}_{j+1/2} = \frac{1}{6}(\mathbf{u}_j + \mathbf{u}_{j+1} + 4\mathbf{u}_{j+1/2})$ , i.e. Simpson's formula.

3. Finally, we state

$$\mathbf{v}_{j+1/2} = \Psi^{-1}(R_{\mathbf{u}}(x_{j+1/2}))$$

In some situations, described later, we will also make the approximation:

$$\mathbf{v}_{j+1/2} = \Psi^{-1}(\bar{\mathbf{u}}_{j+1/2})$$

which is nevertheless consistent. The ODE systems (6) are integrated by a standard ODE solver. We will choose the Euler forward method, and the second order and third order SSP Runge-Kutta scheme.

## 2.2 Analysis of the method

In order to explain why the method can work, we will choose the simplest ODE integrator, namely the Euler forward method. The general case can be done in the same way, with more technical details. So we integrate (6) by:

$$\bar{\mathbf{u}}_{j+1/2}^{n+1} = \bar{\mathbf{u}}_{j+1/2}^n - \frac{\Delta t}{\Delta_{j+1/2}} (\mathbf{f}(\mathbf{u}_{j+1}^n) - \mathbf{f}(\mathbf{u}_j^n)), \quad (7)$$

and

$$\mathbf{v}_j^{n+1} = \mathbf{v}_j^n - \Delta t (\overleftarrow{\Phi}_{j+1/2}^{\mathbf{v}} + \overrightarrow{\Phi}_{j-1/2}^{\mathbf{v}}) \quad (8)$$

Using the transformation (6c), from (8), we can evaluate  $\mathbf{u}_j^{n+1} = \Psi(\mathbf{v}_j^{n+1})$ , and then write

$$|C_j| (\mathbf{u}_j^{n+1} - \mathbf{u}_j^n) + \Delta t \delta \mathbf{u}_{j+1}.$$

The choice of  $|C_j|$  is a bit arbitrary, as well as the definition of the cell  $C_j$ . In order to get some hint about this, we start by Simpson formula, which is exact for quadratic polynomials:

$$\int_{x_j}^{x_{j+1}} f(x) dx \approx \frac{\Delta_{j+1/2}}{6} (f(x_j) + 4f(x_{j+1/2}) + f(x_{j+1})),$$

and then we write for any  $\varphi \in C_0^1(\mathbb{R})$ , and  $C_j = \frac{\Delta_{j+1/2} + \Delta_{j-1/2}}{6}$

$$\begin{aligned} & \sum_{[x_j, x_{j+1}], j \in \mathbb{Z}} \frac{\Delta_{j+1/2}}{6} \left( \varphi_{j+1}(\mathbf{u}_{j+1}^{n+1} - \mathbf{u}_{j+1}^n) + 4\varphi_{j+1/2}(\mathbf{u}_{j+1/2}^{n+1} - \mathbf{u}_{j+1/2}^n) + \varphi_j(\mathbf{u}_j^{n+1} - \mathbf{u}_j^n) \right) \\ &= \sum_{[x_j, x_{j+1}], j \in \mathbb{Z}} \frac{\Delta t}{6} \left( \varphi_{j+1} \delta_{j+1} \mathbf{u}_{j+1}^n + 4\varphi_{j+1/2} \left( \frac{3}{2} \delta_{j+1/2} f - \frac{\delta_{j+1} u + \delta_j u}{4} \right) + \varphi_j \delta_j u^n \right) \\ &= \sum_{[x_j, x_{j+1}], j \in \mathbb{Z}} \Delta t \delta_{j+1/2} f + \sum_{j \in \mathbb{Z}} \Delta t (2\varphi_j - \varphi_{j+1/2} - \varphi_{j-1/2}) \delta_j u \end{aligned}$$

So using classical arguments, we see that if  $\max_{j \in \mathbb{Z}} \|\mathbf{u}_j^n\|_\infty$  and  $\max_{j \in \mathbb{Z}} \|v_{j+1/2}^n\|_\infty$  are bounded, and if a subsequence of  $\mathbf{u}_\Delta$  converges in  $L^1$ , we have that

$$\limsup_{\max \Delta_{j+1/2} \rightarrow 0} \sum_{j \in \mathbb{Z}} \Delta_{j+1/2} \|\delta_j u\| = 0$$

if we assume that there is a Lipschitz continuous dependency of  $\overleftarrow{\Phi}_j^v$  and  $\overrightarrow{\Phi}_j^v$  with respect to  $\mathbf{u}_l$  and  $\mathbf{v}_l$ .

### 3 Some examples of discretisation

We list possible choices: for  $\frac{\partial \mathbf{v}}{\partial t} + J \frac{\partial \mathbf{v}}{\partial x} = 0$ , where  $J$  is the Jacobian of  $f$  with respect to  $\mathbf{u}$ ; they have been used in the numerical tests. The question here is to define  $\overleftarrow{\Phi}_{j+1/2}^v$  and  $\overrightarrow{\Phi}_{j+1/2}^v$  that are the contributions of  $K_{j+\pm 1/2}$  to  $J \frac{\partial \mathbf{v}}{\partial x}$  so that

$$J \frac{\partial \mathbf{v}}{\partial x}(x_i) = \overleftarrow{\Phi}_{j+1/2}^v + \overrightarrow{\Phi}_{i-1/2}^v.$$

We follow the work of Iserle [17] who gives all the possible schemes that guaranty a stable (in  $L^2$ ) semidiscretisation of the convection equation, for a regular grid which we assume. The only difference in his notations and ours is that the grid on which are defined the approximation of the derivative is that composed of the mesh points  $x_j$  and the half points  $x_{j+1/2}$ .

The first list of example have an upwind flavour:

$$\frac{\Delta x}{2} \left( J \frac{\partial v}{\partial x} \right)_j = (J(\mathbf{v}_i))^- \delta_j^- v + (J(\mathbf{v}_i))^+ \delta_j^+ v \quad (9)$$

i.e.

$$\overleftarrow{\Phi}_{j+1/2}^v = (J(\mathbf{v}_i))^- \delta_j^- \mathbf{v} \text{ and } \overrightarrow{\Phi}_{j+1/2}^v = (J(\mathbf{v}_{j+1}))^+ \delta_{j+1}^+ \mathbf{v}$$

where  $\delta_j^\pm$  is a approximation of  $\Delta x \frac{\partial v}{\partial x}$  obtained from [17]:

- First order approximation: we take

$$\delta_j^+ \mathbf{v} = \mathbf{v}_j - \mathbf{v}_{j-1/2}, \quad \delta_j^- \mathbf{v} = \mathbf{v}_{j+1/2} - \mathbf{v}_j.$$

- Second order: We take

$$\begin{aligned} \delta_j^- \mathbf{v} &= -\frac{\mathbf{v}_{j+1/2}}{3} - \frac{\mathbf{v}_{j+1}}{2} + \mathbf{v}_{j+3/2} - \frac{\mathbf{v}_{j+1}}{6} \\ \delta_j^+ \mathbf{v} &= \frac{\mathbf{v}_{j+1/2}}{3} + \frac{\mathbf{v}_j}{2} - \mathbf{v}_{i-1/2} + \frac{\mathbf{v}_{j-1}}{6} \end{aligned}$$

- Third order: The fully centered scheme would be

$$\delta_j \mathbf{v}^\pm = \frac{\mathbf{v}_{i+1} - \mathbf{v}_{i-1}}{12} + 2 \frac{\mathbf{v}_{i+1/2} - \mathbf{v}_{i-1/2}}{3}$$

but we prefer

$$\begin{aligned} \delta_j^- \mathbf{v} &= -\frac{\mathbf{v}_{i-1/2}}{4} - \frac{5}{6} \mathbf{v}_i + \frac{3}{2} \mathbf{v}_{i+1/2} - \frac{\mathbf{v}_{i+1}}{2} + \frac{\mathbf{v}_{i+3/2}}{12} \\ \delta_j^+ \mathbf{v} &= \frac{\mathbf{v}_{i+1/2}}{4} + \frac{5}{6} \mathbf{v}_i - \frac{3}{2} \mathbf{v}_{i-1/2} + \frac{\mathbf{v}_{i-1}}{2} - \frac{\mathbf{v}_{i-3/2}}{12} \end{aligned}$$

- Etc...

It can be useful to have more dissipative versions of a first order scheme. We take:

$$\frac{\Delta x}{2} \left( J \frac{\partial v}{\partial x} \right)_j = \overleftarrow{\Phi}_{j+1/2} + \overrightarrow{\Phi}_{j-1/2}$$

with

$$\begin{aligned} \overleftarrow{\Phi}_{j+1/2} &= \frac{1}{2} J \widehat{\frac{\partial \mathbf{v}}{\partial x}}_j + \alpha \left( \mathbf{v}_j - \frac{\mathbf{v}_j + \mathbf{v}_{j+1/2}}{2} \right) \\ \overrightarrow{\Phi}_{j+1/2} &= \frac{1}{2} J \widehat{\frac{\partial \mathbf{v}}{\partial x}}_{j+1} + \alpha \left( \mathbf{v}_{j+1} - \frac{\mathbf{v}_{j+1} + \mathbf{v}_{j+1/2}}{2} \right) \end{aligned}$$

where  $J \widehat{\frac{\partial v}{\partial x}}_j$  is a constant approximation of  $J \frac{\partial u}{\partial x}$  and  $\alpha$  is an upper-bound of the spectral radius of  $J(\mathbf{v}_j)$ ,  $J(\mathbf{v}_{j+1/2})$  and  $J(\mathbf{v}_{j+1})$ . We take, for simplicity,  $\mathbf{v}_{j+1/2} = \Psi^{-1}(\bar{\mathbf{u}}_{j+1/2})$ . For the model (2), we take

$$J \widehat{\frac{\partial v}{\partial x}}_j = \begin{pmatrix} (\rho u)_{j+1/2} - (\rho u)_j \\ \frac{1}{2}(u_{j+1/2}^2 - u_j^2) + \frac{1}{\tilde{\rho}_{j+1/2}}(p_{j+1/2} - p_j) \\ \tilde{u}_{j+1/2}(p_{j+1/2} - p_j) + \rho c^2(u_{j+1/2} - u_j) \end{pmatrix}$$

where  $\tilde{\rho}_{j+1/2}$  is the geometric average of  $\rho_j$  and  $\rho_{j+1/2}$ ,  $\tilde{u}_{j+1/2}$  is the arithmetic average of  $u_j$  and  $u_{j+1/2}$ , while  $\rho c^2_{j+1/2} = \gamma \frac{p_j + p_{j+1/2}}{2}$ . For the model (3), we take:

$$J \widehat{\frac{\partial v}{\partial x}}_j = \begin{pmatrix} \tilde{u}_{j+1/2}(s_{j+1/2} - s_j) \\ \frac{1}{2}(u_{j+1/2}^2 - u_j^2) + \frac{1}{\tilde{\rho}_{j+1/2}}(p_{j+1/2} - p_j) \\ \tilde{u}_{j+1/2}(p_{j+1/2} - p_j) + \rho c^2(u_{j+1/2} - u_j) \end{pmatrix}.$$

All this has a Local Lax-Friedrichs's flavour, and seems to be positivity preserving for the velocity and the pressure.

Using this, the method is :

$$\frac{\Delta x}{2} \frac{dv_j}{dt} + \overleftarrow{\Phi}_{j+1/2} + \overrightarrow{\Phi}_{j-1/2} = 0 \quad (10a)$$

combined with

$$\Delta x \frac{d\bar{\mathbf{u}}_{j+1/2}}{dt} + \mathbf{f}(\mathbf{u}_{j+1}) - \mathbf{f}(\mathbf{u}_j) = 0. \quad (10b)$$

The system (10) is integrated in time by a Runge-Kutta solver: RK1, RK SSP2 and RK SSP3.

### 3.1 Error analysis in the scalar case

It is easy to check the consistency, and on figure 1 we show the  $L^1$  error on  $u$  and  $\bar{u}$  for (10) with SSPKR2 and SSPRK3 (CFL=0.3) for a convection problem

$$\frac{\partial u}{\partial t} + \frac{\partial u}{\partial x} = 0$$

with periodic boundary conditions and the initial condition  $u_0 = \cos(2\pi x)$ .

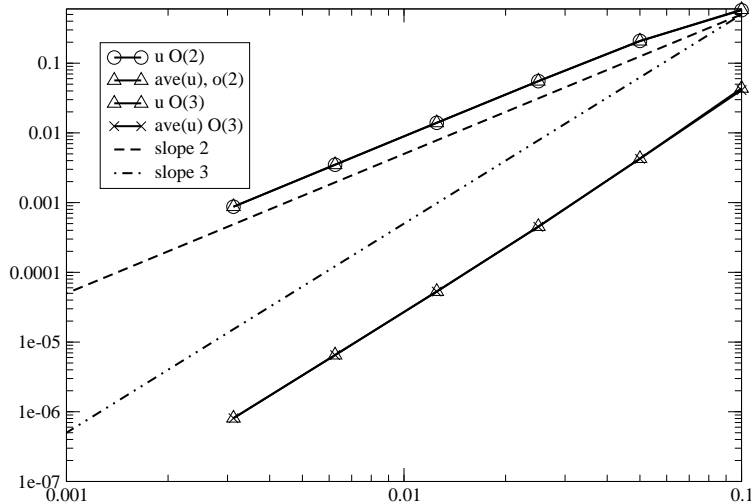


Figure 1: Error plot for  $u$  and  $\bar{u}$  for (10) with SSPKR2 and SSPRK3 (cfl=?). Here  $f(u) = u$ . The second order results are obtained with SSPRK2 with (10a)-(10b), the third order results is obtained by (10a)-(10b).

We also have run this scheme for the Burger equation, and compared it with a standard finite volume (with local Lax-Friedrichs). The conservative form of the PDE is used for the average, and the non conservative one for the point values:  $J = u$  and  $\psi(u) = u$ . This is an experimental check of conservation. The initial condition is

$$\mathbf{u}_0(x) = \sin(2\pi x) + \frac{1}{2}$$

on  $[0, 1]$ , so that there is a moving shock. We can see that the agreement is excellent and that the numerical solution behaves as expected.

### 3.2 Non linear stability

scheme of order  $k$  As such, the scheme is at most linearly stable, with a CFL condition based on the fine grid. However, in case of discontinuities or the occurrence of gradients that are not resolved by the grid, we have to face oscillations, as usual.

So far, it is not very clear how to extend the MUSCL method in this case, so we have relied on the MOOD paradigm [18, 19]. The idea is to work with several schemes ranging from order  $p$  to 1, with the lowest order one able to provide results with positive density and pressure. All schemes,  $S(k)$ ,  $k = 0, \dots, 1$ ,

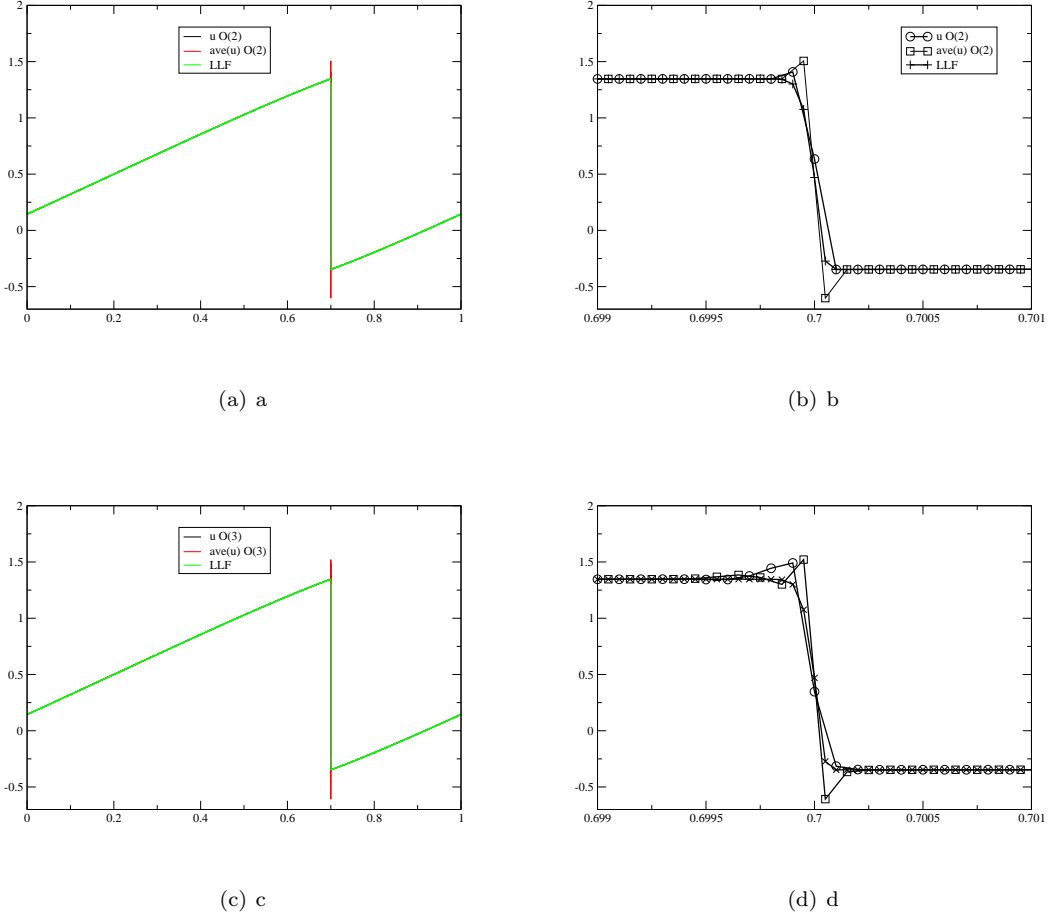


Figure 2: Solution of Burger with 10 000 points,  $t_{fin} = 0.4$ ,  $CFL = 0.4$  for the second order (a and b) ((10a)-(10b) with SSPRK2) and third order (c and d) ((10a)-(10b) with SSPRK3). The global solution is represented in (a) and (c), and a zoom around the discontinuity is shown in (b) and (c).

are assumed to work for a given CFL range, and the algorithm is as follows: For each Runge-Kutta sub-step, starting from  $U^n = \{\bar{u}_{j+1/2}^n, \bar{v}_j^n\}_{j \in \mathbb{Z}}$ , we compute

$$\begin{aligned}
 \tilde{u}_{j+1/2}^{n+1} &= \bar{u}_{j+1/2}^n - \lambda(\mathbf{f}(\mathbf{u}_{j+1}^n) - \mathbf{f}(\mathbf{u}_j^n)) \\
 \tilde{\mathbf{v}}_j^{n+1} &= \tilde{\mathbf{v}}_j^n - 2\lambda \overleftarrow{\Phi}_{j+1/2} \mathbf{v}_{j+1/2} \\
 \tilde{\mathbf{v}}_{j+1}^{n+1} &= \tilde{\mathbf{v}}_{j+1}^n - 2\lambda \overrightarrow{\Phi}_{j+1/2} \mathbf{v}_{j+1/2}
 \end{aligned} \tag{11}$$

by the scheme  $S(p)$ . Then we test the validity of these results in the interval  $x_j, x_{j+1}]$  for the density (and possibly the pressure). This is described a little bit later. The variable  $\mathbf{v}$  is updated as in (11), because at  $t_{n+1}$ , the true update of  $\mathbf{v}_j$  is the half sum of  $\tilde{\mathbf{v}}_j^{n+1}$  and  $\tilde{\mathbf{v}}_{j+1}^{n+1}$ .

If the test is positive, then we keep the scheme  $S(p)$  in that interval, else we start again with  $S(p-1)$ , and repeat the procedure unless all the  $K_{j+1/2}$  have successfully passed the test. This is described in Algorithm 1.



---

**Algorithm 1** Description of the MOOD loop

---

**Require:**  $U^n = \{\bar{u}_{j+1/2}^n, \bar{v}_j^n\}_{j \in \mathbb{Z}}$

**Require:** Allocate  $\{S(j+1/2)\}_{j \in \mathbb{Z}}$  an array of integers. It is initialized with  $S(j+1/2) = p$ .

```
for  $k = p, \dots, 2$  do
  for all For all  $K_{j+1/2}$  do
    Define  $\tilde{\mathbf{u}}_{j+1/2}^{n+1}$ ,  $\tilde{\mathbf{v}}_j^{n+1}$  and  $\tilde{\mathbf{v}}_{j+1}^{n+1}$  as in (11)
    Apply the test on  $\tilde{\mathbf{u}}_{j+1/2}^{n+1}$ ,  $\tilde{\mathbf{v}}_j^{n+1}$  and  $\tilde{\mathbf{v}}_{j+1}^{n+1}$  :
    if test=.true. then
       $S(j+1/2) = k - 1$ 
    end if
  end for
end for
```

---

Now, we describe the tests. We do, in the following order, for each element  $K_{j+1/2}$ , at the iteration  $k > 0$  of the loop of 1: the tests are performed on variables evaluated from  $\mathbf{u}$  and  $\mathbf{v}$ . For the scalar case, they are simply the point values at  $x_j, x_{j+1/2}$  and  $x_{j+1}$ . For the Euler equations they are the density, and possibly the pressure

1. We check if all the variables are numbers (i.e. not NaN). If so, we state that  $S(j+1/2) = k - 1$ ,
2. (Only for the Euler equations) We check if the density is positive. We can also request to check if the pressure is also positive. If the variable is negative, the we state that  $S(j+1/2) = k - 1$ .
3. Then we check if at  $t_n$ , the solution was not constant in the numerical stencils of the degrees of freedom in  $K_{j+1}$ , this in order to avoid to detect a fake maximum principle. We follow the procedure of [19]. if we observe that the solution was locally constant, the  $S(j+1/2)$  is not modified.
4. Then we apply a discrete maximum principle, even for systems though it is not very rigorous. For the variable  $\xi$  (in practice the density, and we may request to do the same on the pressure), we compute  $\min_{j+1/2} \xi$  (resp.  $\max_{j+1/2} \xi$ ) the minimum (resp. maximum) of the values of  $\xi$  on  $K_{j+1/2}, K_{j-1/2}$  and  $K_{j+3/2}$ . We say we have a potentioan maximum if  $\tilde{\xi}^{n+1} \notin [\min_{j+1/2} \xi^n + \epsilon_{j+1/2}, \max_{j+1/2} \xi^n - \epsilon_{j+1/2}]$ , with  $\epsilon_{j+1/2}$  estimated as in [18]. Then:
  - If  $\tilde{\xi}^{n+1} \in [\min_{j+1/2} \xi^n + \epsilon_{j+1/2}, \max_{j+1/2} \xi^n - \epsilon_{j+1/2}]$ ,  $S(j+1/2)$  is not modified
  - Else we use the following procedure introduced in [19]. In each  $K_{l+1/2}$ , we can evaluate a quadratic polynomial  $p_{l+1/2}$  that interolates  $\xi$ . Note that its derivative is linear in  $\xi$ . We compute

$$p'_{j-1/2}(x_j), p'_{j+3/2}(x_{j+1}), p'_{j+1/2}(x_j) \text{ and } p'_{j+1/2}(x_{j+1}).$$

– If

$$p'_{j+1/2}(x_j) \in [\min(p'_{j-1/2}(x_j), p'_{j+3/2}(x_{j+1}))] \text{ and } p'_{j+1/2}(x_{j+1}) \in [\min(p'_{j-1/2}(x_j), p'_{j+3/2}(x_{j+1}))]$$

we say it is a true regular extrema and  $S(j+1/2)$  will not be modified,

– Else the extrema is declared not to be regular, and  $S(j+1/2) = k - 1$

As a first application, to show that the oscilations are well controlled without sacrificyng the accuracy, we consider the advection problem (with constant speed unity) on  $[0, 1]$ , periodic boundary conditions with initial condition:

$$u_0(x) = \begin{cases} 0 & \text{if } y \in [-1, -0.8[ \\ \frac{1}{6}(G(y, \beta, z - \delta) + G(y, \beta, z + \delta) + 4G(y, \beta, z)) & \text{if } y \in [-0.8, -0.6] \\ 1 & \text{if } y \in [-0.4, -0.2] \\ 1 - |10y - 1| & \text{if } y \in [0, 0.2] \\ \frac{1}{6}(F(y, \beta, z - \delta) + G(y, \beta, z + \delta) + 4F(y, \beta, z)) & \text{else,} \end{cases} \quad \text{with } y = 2x - 1$$

Here  $a = 0.5$ ,  $z = -0.7$ ,  $\delta = 0.005$ ,  $\alpha = 10$ ,

$$\beta = \frac{\log 2}{36\delta^2}$$

and

$$G(t, \beta, z) = \exp(-\beta(t-z)^2), \quad F(t, a, \alpha) = \sqrt{\max(0, 1 - \alpha(t-a)^2)}.$$

The results are obtained for 200 points and are very reasonable.

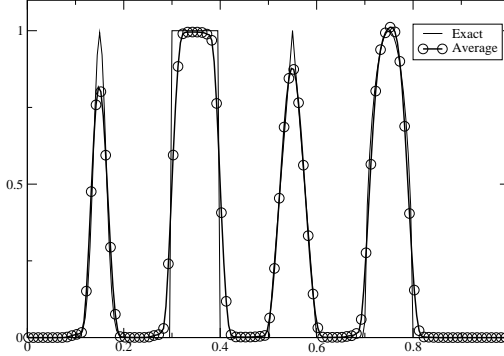


Figure 3: Shu Jiang problem, CFL=0.4, third order scheme, 200 points, periodic conditions. The point values and cell average are almost undistinguishable.

## 4 Numerical results for the Euler equations

In this section, we show the flexibility of the approach, where conservation is recovered only by the equation (10a), and so lots of flexibility is possible with the relations on the  $\mathbf{u}_i$ . To illustrate this, we consider the Euler equations. We will consider the conservative formulation (1) for the average value, so  $\mathbf{u} = (\rho, \rho u, E)^T$  and either the form (2), i.e.  $\mathbf{v} = (\rho, u, p)$  or the form (3) with  $\mathbf{v} = (p, u, s)^T$ .

### 4.1 Sod with moderate resolution

The Sod case is defined for  $[0, 1]$ , the initial condition is

$$(\rho, u, p)^T = \begin{cases} (1, 0, 1)^T & \text{for } x < 0.5 \\ (0.125, 0, 0.1)^T & \text{else.} \end{cases}$$

The final time is  $T = 0.16$ . The problem is solved with (1)-(2) and displayed in figures 4, 5, 6 and 7, while the solution obtained with the combination (1)-(3) is shown on figure 8 and (9). When the MOOD procedure is on, it is applied with  $\rho$  and  $p$  and all the test are performed. The exact solution is also shown every time. Different order in time/space are tested. The results are good, eventhough the MOOD procedure is not perfect. This the use of the combination (1)-(3) seems more challenging, we have performed a convergence study (with 10000 points). This is shown on figure (9), and a zoom around the contact discontinuity is also shown.

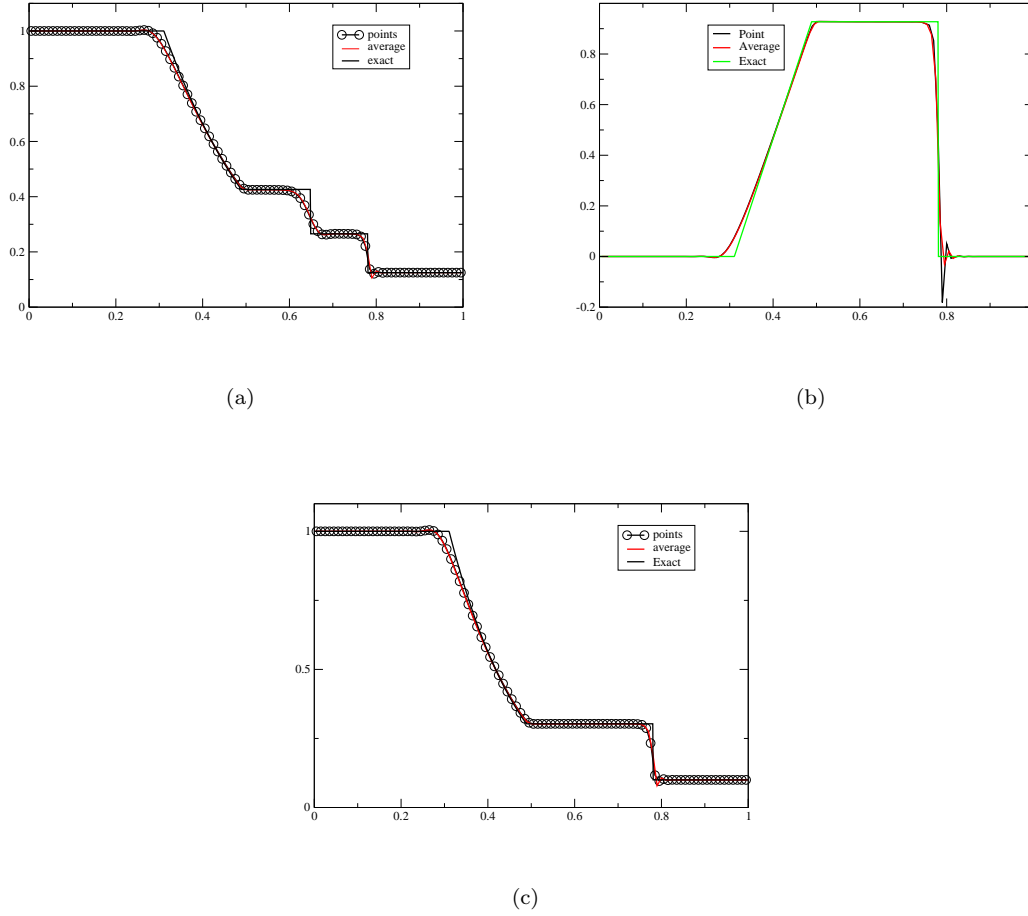


Figure 4: 100 grid points, and the third order SSPRK2 scheme with CFL=0.1. (a): density, (b): velocity, (c): pressure.

## 4.2 Shu-Osher case

The initial condition are:

$$(\rho, u, p) = \begin{cases} (3.857143, 2.629369, 10.3333333) & \text{if } x < -4 \\ (1 + 0.2 \sin(5x), 0, 1) & \text{else} \end{cases}$$

on the domain  $[-5, 5]$  until  $T = 1.8$ . We have used the combination (1)-(2), since the other one seems less robust. The density is compared to a reference solution (obtained with a standard finite volume scheme with 20 000 points, and the solution obtained with the third order scheme with  $CFL = 0.3$  and 200, 400, 800 and 1600 points. The mood procedure uses the first order upwind scheme if a PAD, a NaN or DMP is detected, the other cases use the 3rd order scheme. The CFL is that small because the scheme has no positivity property. The solutions are displayed in 10. With little resolution, the results are very close of the reference one. For figure reffigshu, the second order scheme is used as a rescue scheme.

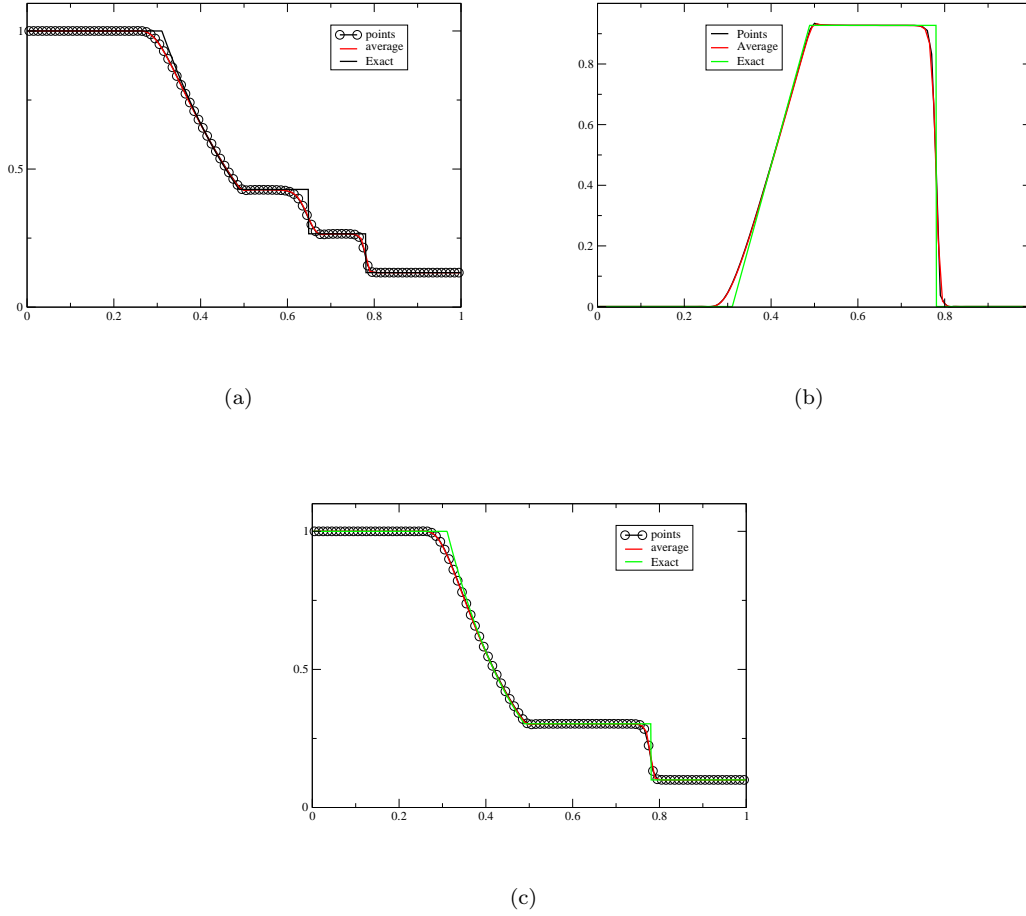


Figure 5: 100 grid points, and the third order SSPRK2 scheme with CFL=0.1. (a): density, (b): velocity, (c): pressure. Test made on  $\rho$  and  $p$

### 4.3 Le Blanc case

The initial conditions are

$$(\rho, u, e) = \begin{cases} (1, 0, 0.1) & \text{if } x \in [-3, 3] \\ (0.001, 0.10^{-7}) & \text{if } x \in [3, 6] \end{cases}$$

where  $e = (\gamma - 1)p$  and  $\gamma = \frac{5}{3}$ . The final time is  $t = 6$ . This is a very strong shock tube. The combination (1)-(2). It is not possible to run higher than first order without the MOOD procedure. We show the second and third order results are shown on figure 11.

At time  $t = 6$  the shock wave should be at  $x = 8$ : in addition to the extreme conditions, it is generally difficult to get a correct position of the shock wave; this is why a convergence study is shown in figure 12. It is performed with 400, 800, 10000 grid points, and the third order SSPRK3 scheme with CFL=0.1. It is compared to the exact solution

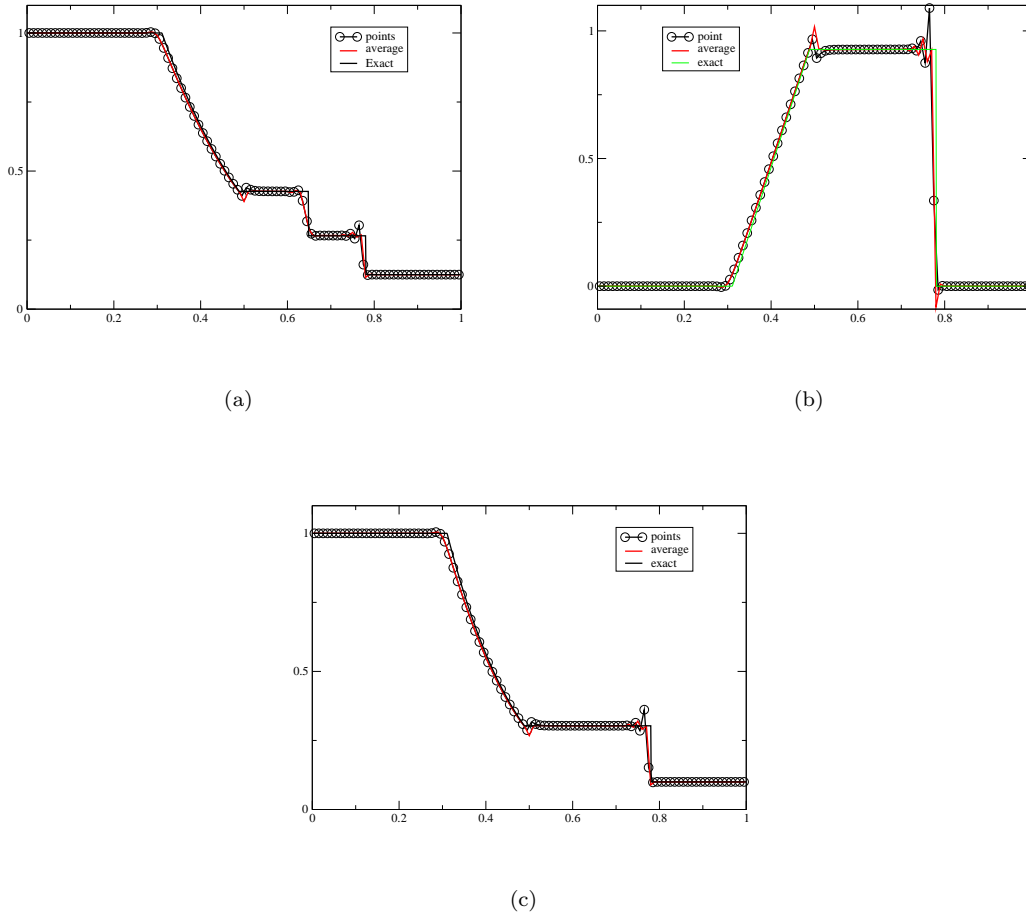


Figure 6: 100 grid points, and the third order SSPRK3 scheme with CFL=0.1. (a): density, (b): velocity, (c): pressure.

## 5 Conclusion

This study is preliminary and should be seen as a proof of concept. We show how to combine, without any test, several formulations of the same problem, one conservative and the other ones in non conservative form, in order to compute the solution of hyperbolic systems. The emphasis is mostly put on the Euler equation.

We explain why the formulation lead to a method that satisfies a Lax-Wendroff like theorem. We also propose a way to provide non linearity stability, this method works well but is not yet completely satisfactory.

Besides the theoretical results, we also show numerically that we get the convergence to the correct weak solution. This is done on standard bench mark, some being very challenging.

We intend to extend the method to several space dimension, and improve the limiting strategy. Different systems, such as the shallow water system, will also be considered.

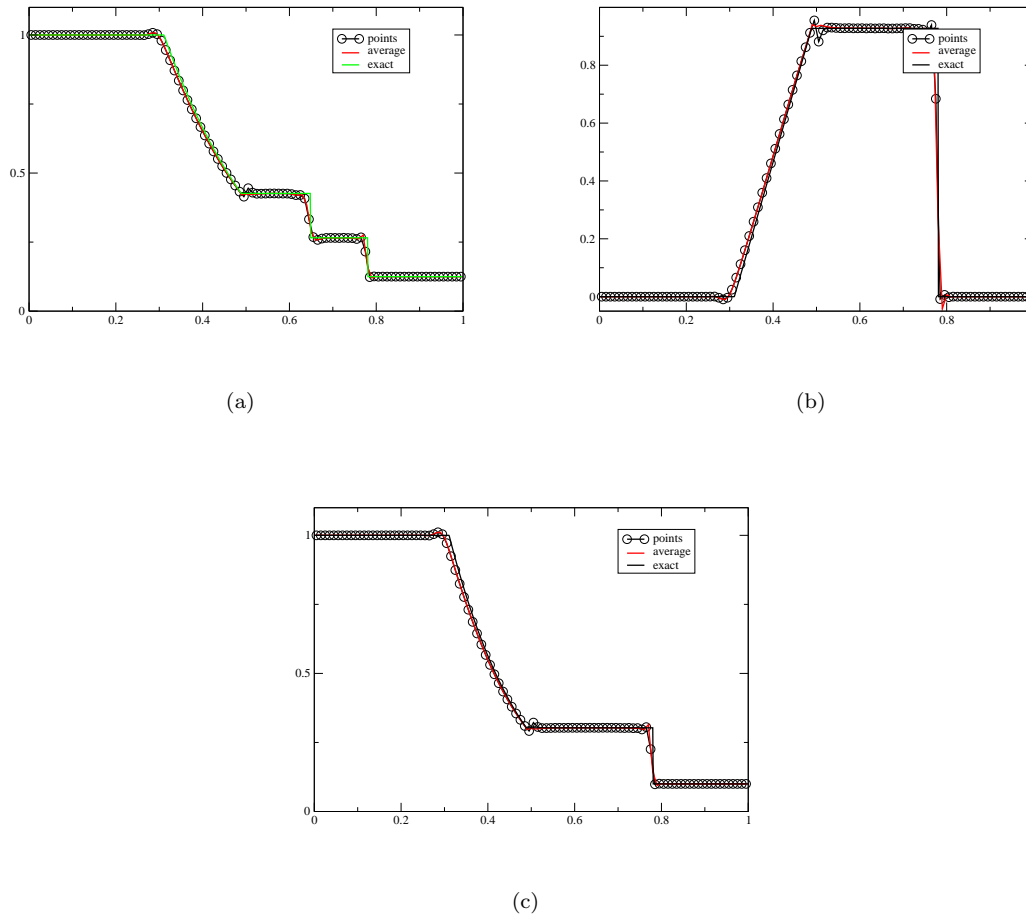


Figure 7: 100 grid points, and the third order SSPRK3 scheme with CFL=0.1. (a): density, (b): velocity, (c): pressure. Mood Test made on  $\rho$  and  $p$

## References

- [1] P. Lax and B. Wendroff. Systems of conservation laws. *Comm. Pure Appl. Math.*, 13:381–394, 1960.
- [2] T. Y. Hou and P. G. Le Floch. Why nonconservative schemes converge to wrong solutions : error analysis. *Math. Comp.*, 62(206):497–530, 1994.
- [3] Veselin A. Dobrev, Tzanio V. Kolev, and Robert N. Rieben. High-order curvilinear finite element methods for Lagrangian hydrodynamics. *SIAM J. Sci. Comput.*, 34(5):B606–B641, 2012.
- [4] Rémi Abgrall and Svetlana Tokareva. Staggered grid residual distribution scheme for Lagrangian hydrodynamics. *SIAM J. Sci. Comput.*, 39(5):A2317–A2344, 2017.
- [5] Rémi Abgrall, Konstantin Lipnikov, Nathaniel Morgan, and Svetlana Tokareva. Multidimensional staggered grid residual distribution scheme for Lagrangian hydrodynamics. *SIAM J. Sci. Comput.*, 42(1):A343–A370, 2020.

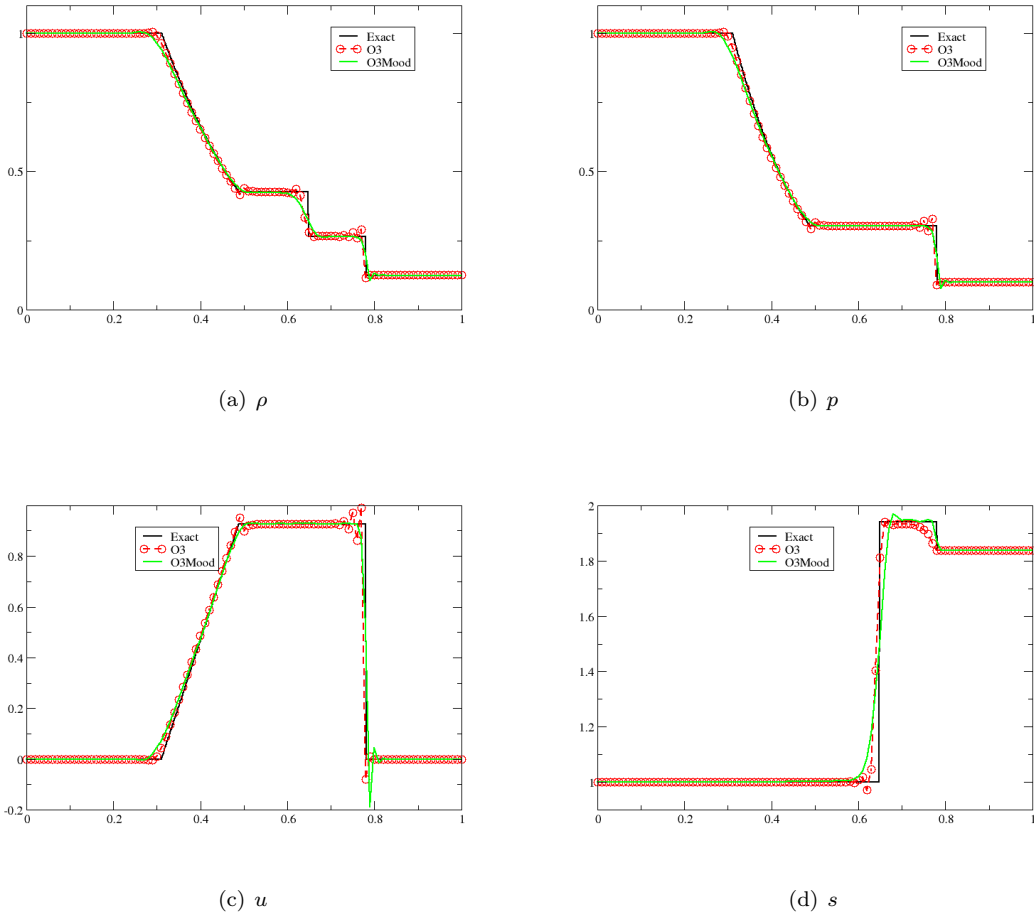
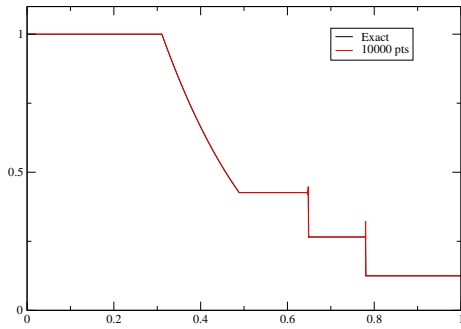


Figure 8: Solution with the variables  $(s,u,p)$  for 100 points, comparison with the exact solution, third order in time/space with Mood and non Mood. Mood is done on  $\rho$  and  $p$ .  $Cfl=0.2$

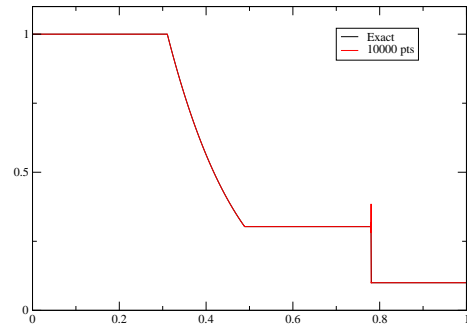
- [6] Raphaële Herbin, Jean-Claude Latché, and Trung Tan Nguyen. Consistent segregated staggered schemes with explicit steps for the isentropic and full Euler equations. *ESAIM Math. Model. Numer. Anal.*, 52(3):893–944, 2018.
- [7] Gautier Dakin, Bruno Després, and Stéphane Jaouen. High-order staggered schemes for compressible hydrodynamics. Weak consistency and numerical validation. *J. Comput. Phys.*, 376:339–364, 2019.
- [8] R. Abgrall and K. Ivanova. High order schemes for compressible flow problems with staggered grids. in preparation, 2020.
- [9] Rémi Abgrall, Paola Bacigaluppi, and Svetlana Tokareva. High-order residual distribution scheme for the time-dependent Euler equations of fluid dynamics. *Comput. Math. Appl.*, 78(2):274–297, 2019.
- [10] Rémi Abgrall. Some remarks about conservation for residual distribution schemes. *Comput. Methods Appl. Math.*, 18(3):327–351, 2018.

- [11] Smadar Karni. Multicomponent flow calculations by a consistent primitive algorithm. *J. Comput. Phys.*, 112(1):31–43, 1994.
- [12] T.A. Eyman and P.L. Roe. Active flux. 49th AIAA Aerospace Science Meeting, 2011.
- [13] T.A. Eyman and P.L. Roe. Active flux for systems. 20 th AIAA Computational Fluid Dynamics Conference, 2011.
- [14] T.A. Eyman. *Active flux*. PhD thesis, University of Michigan, 2013.
- [15] C. Helzel, D. Kerkmann, and L. Scandurra. A new order method inspired by the active flux method. *Journal of Scientific Computing*, 80(3):35–61, 2019.
- [16] W. Barsukov. The active flux for system. <https://arxiv.org/pdf/2011.10056.pdf>, 2020.
- [17] A. Iserles. Order stars and saturation theorem for first-order hyperbolics. *IMA J. Numer. Anal.*, 2:49–61, 1982.
- [18] S. Clain, S. Diot, and R. Loubère. A high-order finite volume method for systems of conservation laws—Multi-dimensional Optimal Order Detection (MOOD). *J. Comput. Phys.*, 230(10):4028–4050, 2011.
- [19] François Vilar. *A posteriori* correction of high-order discontinuous Galerkin scheme through subcell finite volume formulation and flux reconstruction. *J. Comput. Phys.*, 387:245–279, 2019.

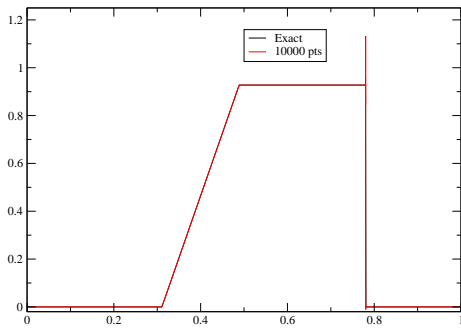




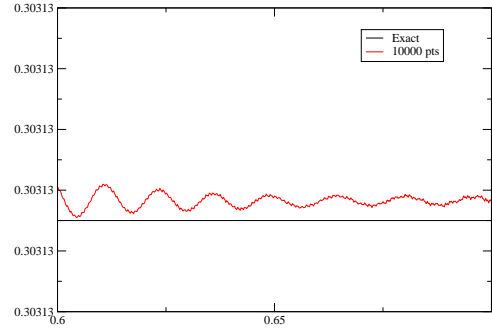
(a)  $\rho$



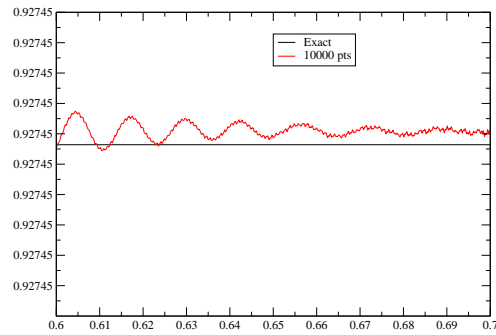
(b)  $p$



(c)  $u$

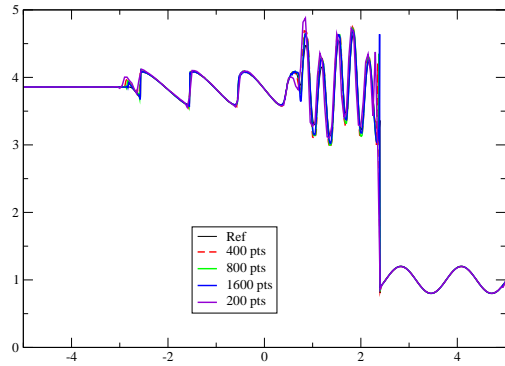


(d)  $p$  zoom

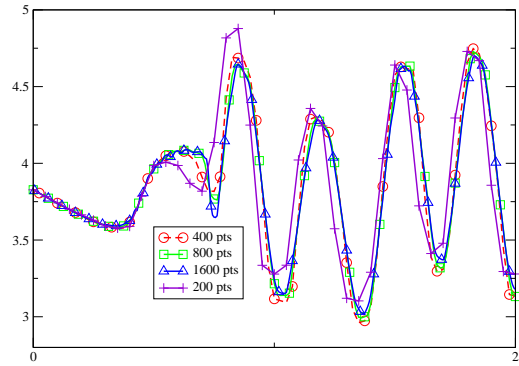


(e)  $u$  zoom

Figure 9: Solution with the variables  $(s,u,p)$  for 10000 points, comparison with the exact solution.  $Cfl=0.1$ , no mood The zoomed figures are for  $x \in [0.6, 0.7]$  and the ticks are for  $10^{-7}$ . We plot  $u$  and  $p$  across the contact

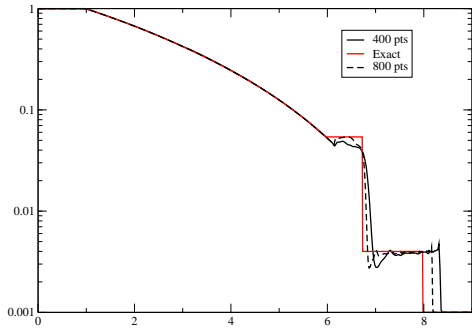


(a)

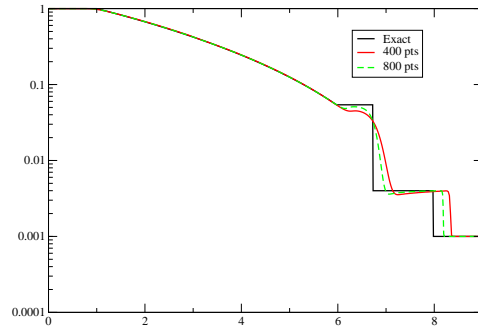


(b)

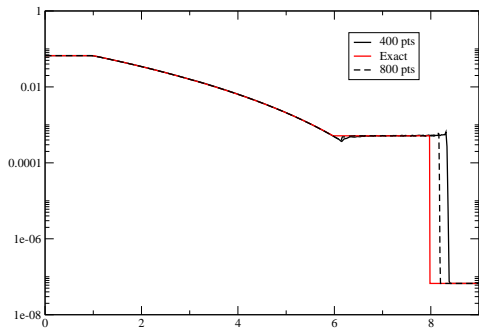
Figure 10: (a): Solution of the Shu Osher problem , (b): zoom of the solution around the shock.



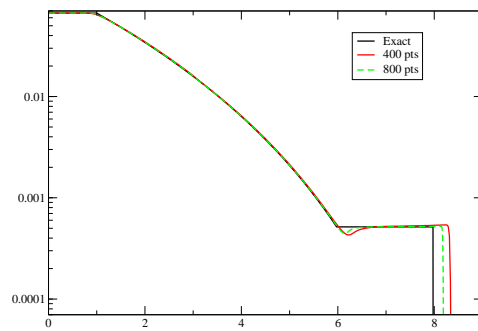
(a)



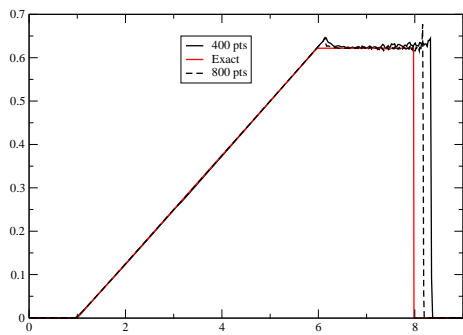
(b)



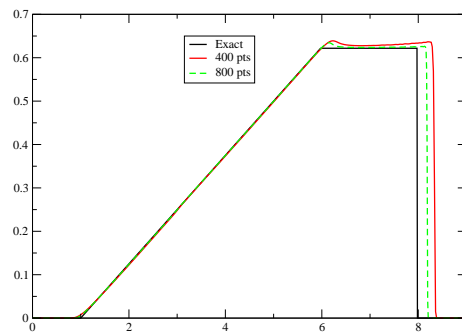
(c)



(d)

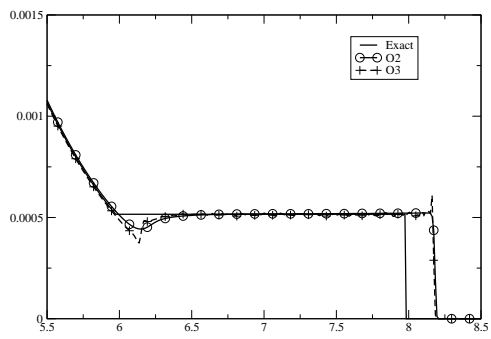


(e)

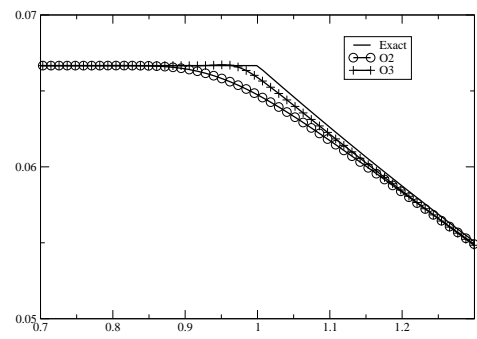


(f)

Figure 11: Le Blanc test case,  $cfi=0.1$ , from 400 to 800 points.

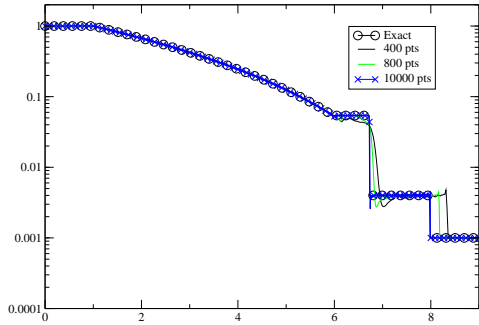


(a)

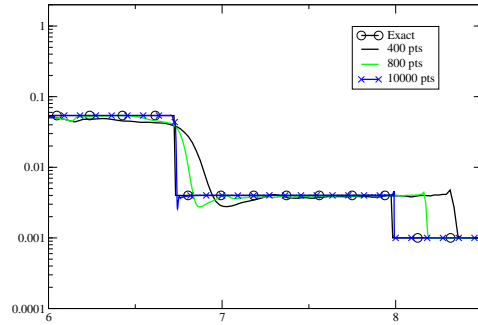


(b)

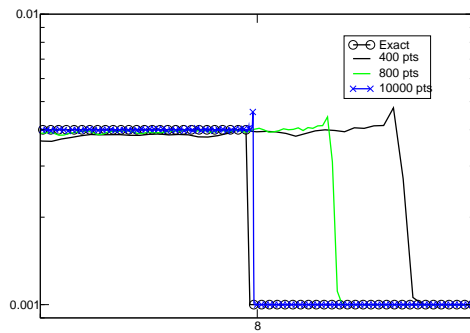
Figure 12: Le Blanc test case, zooms



(a)



(b)



(c)

Figure 13: Convergence study for the LeBlanc test case.